REGULAR AND STOCHASTIC DYNAMICS IN A CYCLOTRON-MASER ACCELERATOR*

R. PAKTER, G. CORSO, T. S. CAETANO, D. DILLENBURG and F. B. RIZZATO
Instituto de Física - Universidade Federal do Rio Grande do Sul
Caixa Postal 15051
91501-970 Porto Alegre, RS, Brasil

Abstract

We develop a self-consistent, nonperturbative Hamiltonian formulation for the Cyclotron-Resonance laser accelerator where magnetized electrons are accelerated by circularly polarized laser modes. Wave dispersion and frequency mismatch are taken into account, enabling one to show how the mismatch can be used to remove some of the energization limits imposer by dispersion. We make use of an analytical macroparticle (or bunching) approximation which is shown to be accurate when the initial energy of the accelerating particles es small enough. Wave-particle numerical simulations are used to precisely establish the validity of that approximation. Beyond these limits, bifurcated periodic orbits and chaotic motion characterized both by resonance overlap and positive Lyapunov exponents are shown to occur.

1 INTRODUCTION

A promising configuration for laser acceleration is the so called cyclotron-resonance laser accelerator (CRLA), where a coherent electromagnetic wave may transfer a large amount of energy to a beam of electrons gyrating in a guide magnetic field. This large amount of transferred energy takes place because of the autoresonance mechanism [1, 2] where, under some ideal conditions, an initial wave-particle synchronism is self-sustained throughout the accelerating period.

It has been observed, however, that one of these CRLA ideal conditions is hardly obtained in feasible experimental schemes. This particular condition is the one requiring the laser field to be *dispersionless* [3, 4], a very restrictive condition if one takes into account dispersive effects arising from the confining wave guides [5].

In the present work we perform an improved analysis of the mentioned self-consistent wave-particle interaction, taking into account a possible frequency mismatch between wave and particles. We will show how the frequency mismatch can compensate the dispersion effects. Moreover, we numerically integrate the motion equations of a large number of electrons interacting self-consistently with the wave in order to test the efficiency of the particles phase space bunching process that is supposed to occur[3]. We show that for *small* initial energies this process effectively takes place, validating theoretical predictions. Otherwise, a total spread is found and chaotic trajectories may arise. The onset of chaos is studied by means of bifurcation theory.

2 SELF-CONSISTENT HAMILTONIAN FORMALISM

Let us consider an electron beam and a circularly polarized electromagnetic wave, co-propagating along the homogeneously magnetized $\mathbf{z}$ axis of the chosen reference frame.

The circularly polarized wave vector potential is written as $\frac{e}{mc^2}\mathbf{A} \equiv -\frac{1}{2}\sqrt{\rho}\, e^{i\sigma}\, e^{i\hat{\omega}\,(fz-t)}\,\hat{e}_c + c.c.$ where ρ and σ have a slow time dependence, e is the electron charge, $\hat{e}_c \equiv \hat{\mathbf{x}} + i\hat{\mathbf{y}}$ and $\hat{\omega} \equiv \omega/\omega_{co}$. The variable ω is the wave frequency satisfying a dispersion relation of the form $\omega/ck = \sqrt{1+g^2} \equiv f^{-1} \geq 1$ with g as a factor accounting for dispersion (it could be a factor connected with the finite transverse dimensions of some guiding system) and k is the wave vector. We introduce $\omega_{co} \equiv |e|B_{z,o}/mc$ with $B_{z,o}$ as the background magnetic field and normalize time and space to ω_{co} and ω_{co}/c respectively.

The slow time self-consistent evolution equation for the amplitude of the vector potential is readily derived from Maxwell's equations. Using the so-called macroparticle approximation [3], that assumes an extreme bunching condition for which the wave-particle relative phase $\phi_i + \hat{\omega}(f\,z_i - t)$ is the same for all particles it becomes possible to write the evolution equation for ρ and σ[4]:

$$d_t\rho = -2\omega_p^2\frac{\sqrt{2\,I}}{2\Gamma}\sqrt{\rho}\,sin(\phi+\sigma), \qquad (1)$$

and

$$-\;d_t\sigma = \omega_p^2\frac{\sqrt{2\,I}}{2\Gamma}\;\frac{1}{\sqrt{\rho}}\,cos(\phi+\sigma) + \frac{\omega_p^2}{2\,\Gamma}. \qquad (2)$$

where $\omega_p^2 \equiv 4\pi e^2 N/mV\; m\omega\omega_{co}$, with N as the number of particles.

Now, if one re-scales ρ according to $\rho = \lambda\hat{\rho}$ with $\lambda \equiv \omega_p^2$, the interesting and final conclusion is that *all* the relevant dynamical equations for both particles *and* fields can be derived from one generalized Hamiltonian given by

$$\begin{aligned}\mathcal{H} \;&=\; [1 + 2I + P_z^2 + \lambda\,\hat{\rho}\,+ \\ &\quad 2\sqrt{2\,I\,\lambda\,\hat{\rho}}\,\cos(\phi + \hat{\omega}(f\,z_i - t) - \sigma')]^{1/2}, \qquad (3)\end{aligned}$$

where I and ϕ are the guiding-center variables corresponding to electronic motion, $\hat{\rho}$ is the "momentum" corresponding to the wave field and σ' $(= -\sigma)$ is its canonically conjugated co-ordinate.

*Work supported by CNPq and FINEP. Numerical Calculations done on the CRAY YMP-2E at the Super Computing Center - UFRGS.

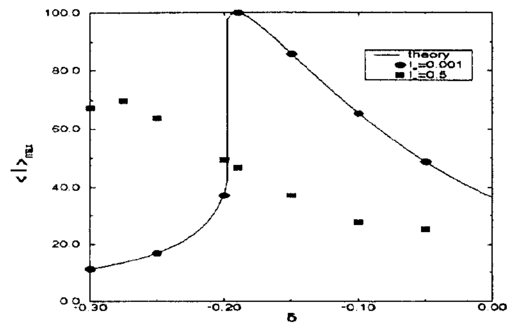

Figure 1: maximum energization vs. δ for $\lambda\rho = 1$ and $f = 0.9$

Now we write $\hat{\omega} = \omega' + \delta$, with $\omega' = (1+\rho)^{-1/2}$ as the exact resonant condition($\omega = \omega_{co}/\gamma + kv_z$) for $I(t=0) = P_z(t=0) = 0$, and δ a small mismatch parameter. In order to make the Hamiltonian simpler we can introduce the canonical transformations $\phi\ + (\omega' + \delta) f z - \omega' t \rightarrow \phi$, $P_z \rightarrow P_z + f(\omega' + \delta) I$, $\sigma' + \delta t \rightarrow \sigma'$ and $\mathcal{H} \rightarrow \mathcal{H} - \omega' I + \delta\rho$. Besides, the adittional canonical transformations $\phi - \sigma' = \phi'$ and $\hat{\rho} = \rho_c - I$ reduces the degrees of freedom (ρ_c is a constant of motion) and allows to write a final effective canonical system $\mathcal{H} = -\hat{\omega}\, I + \delta(\rho_c - I) + \Gamma$, with

$$\Gamma = [1 + 2I + [P_z + (\omega' + \delta)\, f\, I]^2 + \lambda\,(\rho_c - I) + 2\sqrt{2\, I\, \lambda\,(\rho_c - I)}\,\cos\phi]^{1/2},$$

and $d_t I = -\partial_\phi \mathcal{H}$, $d_t \phi = \partial_I \mathcal{H}$.

To evaluate the maximum energization, I_{max} (since I is proportional to the energy Γ in view of the fact that H is now a constant of motion), it is possible to combine our canonical equations to obtain a closed equation for I[4]

In figure 1 it is shown the maximum energization vs. δ (solid line) for a typical case which lies in the microwave range, with a frequency of the order of $10 - 10^2 GHz$ and a tenuous beam of density $\sim 10^9 cm^{-3}$ in order to define a small $\lambda = 0.01$. As we can see, a judicious choice of δ enables the particles to reach energies approximately six times larger than in the exact resonant case($\delta = 0$).

3 NUMERICAL SIMULATION

In order to verify the validity of the macroparticle approximation for mismatched systems we perform a numerical integration of 500 electrons in the cyclotron-resonance laser accelerator[6]. All the electrons are supposed to initially have the same action and to be homogeneously distributed along $0 < \phi < 2\pi$.

In figure 1 we plot the maximum energization(I_{max}) vs. the mismatch(δ). Solid lines represent macroparticle results while symbols represent simulations with $I_o = 0.001$ (circles) and $I_o = 0.5$ (squares). One is able to see that for a small initial energy phase bunching effectively occurs and we have a good agreement between theory and simulation. On the other hand, in the case $I_o = 0.5$ the agreement is poor, and the maximum possible acceleration(around $\delta = -0.35$) is highly reduced.

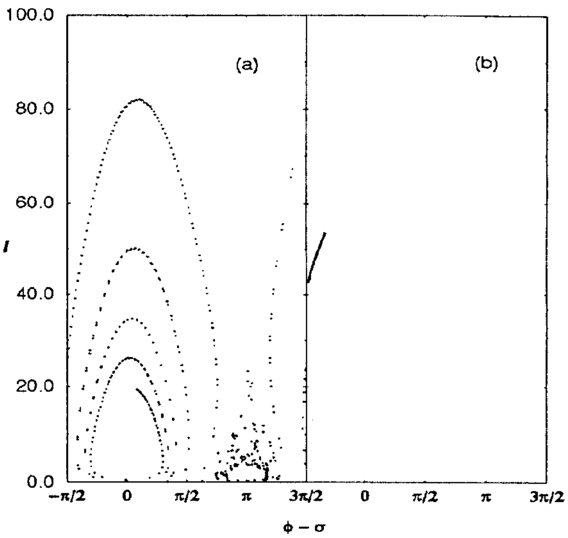

Figure 2: comparision of particles phase space after 1000 waves cycles for $\delta = -0.1$ and (a) $I_o = 0.5$; (b) $I_o = 0.001$

In figures 2 it is compared the phase-space after 1000 wave cycles of the cases $I_o = 0.5$ (a) and $I_o = 0.001$ (b). Once again, it is seen that phase bunching does not occur for too large values of the action. Furthermore, we can see a chaotic distribution of particles surrounding the eliptic fixed point at $\phi = \pi$, what indicates that acceleration can also occur due to stochastic diffusion in those cases of weak bunching.

4 TRANSITION TO CHAOS

Given that regular acceleration may not be always dominant in a CRMA, an issue to be addressed would be the possibility of stochastic acceleration. This could be the governing accelerating mechanism when beam control is poor or even absent. Such is the case of astrophysical beams in pulsar magnetospheres, for instance, where the usual wave-particle model is identical to the one we shall making use of[7]. The analysis is also relevant for laboratory schemes where the accelerating length is long enough such that the effect of long range inhomogeneities can not be left aside. The problem with stochastic processes, as mentioned before, is that constant amplitude modes generates only regular trajectories. One should note, however, that slow amplitude modulations may easily develop in this kind of system because of various factors. Among these, at least three can be considered as of relevance. (i) Low energy particles, even if in small number, interact with the wave and cause pump depletion, so that higher energy particles will view the resulting wave as a modulated train[6] (ii) Electromagnetic waves are unstable and can frequently develop nonlinear amplitude self-modulations[7] (iii) Slow modulations on the wave can be produced in laboratories

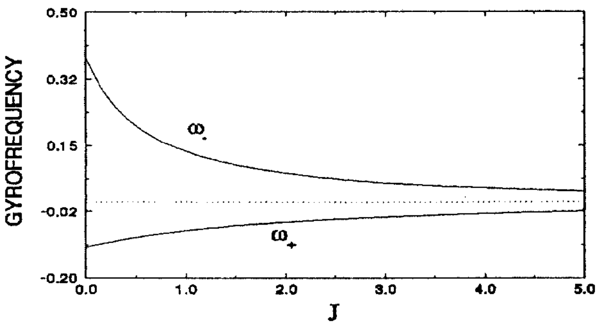

Figure 3: comparision of particles phase space after 1000 waves cycles for $\delta = -0.1$ and (a) $I_o = 0.5$; (b) $I_o = 0.001$

by slowly varying control parameters in an experiment. We shall show that wave modulation, no matter its precise origin, may indeed be responsible for the development of bifurcations and stochastization of periodic orbits in cyclotron-maser systems.

An appropriate resonance analysis involves the calculation of particle gyrofrequencies. These gyrofrequencies should be fully renormalized by the presence of the large-amplitude maser modes and can be derived for the exactly integrable case where the Hamiltonian is a conserved quantity, $\mathcal{H}_o \rightarrow \mathcal{H}(I, \phi, \rho = \rho_o) \equiv E$ by introducing an action variable J according to[8]

$$J = \frac{1}{2\pi} \oint I(E, \phi)\, d\phi. \tag{4}$$

Inverting the above equation we can write $\mathcal{H}_o = \mathcal{H}_o(J)$. By setting $J = 0$, we find the central fixed points $CFP_{\pm}$ corresponding to the co-ordinates $(\phi_{\pm}, I_{\pm})$, given by $\cos\phi_{\pm} = \pm 1$ and $\partial_I \mathcal{H}_1(\phi_{\pm}, I_{\pm}) = 0$. The renormalized gyrofrequencies for orbits around the fixed points, $\omega_{\pm}$, are obtained as functions of J from $\omega_{\pm} = \partial_J \mathcal{H}_{o,\pm}$ and are plotted in Fig. 3. It is seen that the gyrofrequencies decrease with J. This means that primary resonances located at J_n $(n = \pm 1, \pm 2, ...)$ with $n\omega_{\pm}(J_n) = \Omega$ and secondary resonances located at $J_{n,p}$ with $n\omega_{\pm}(J_{n,p}) = p\,\Omega$. and $p \neq \pm 1$, are such that larger $n's$ correspond to larger $J_{n,p}$ $'s$. As we shall be assuming $\omega_{\pm}(J = 0) > \Omega$, this implies that for both branches the lower primary resonance present in the system will be the one with $|n| = 1$. Elliptic points of a $J_{n,p}$ resonance shall be denoted as $(J_{n,p})_e$ and hyperbolic points as $(J_{n,p})_h$.

Attention is focused on primary resonances generating trajectories with the same period as the modulation when the modulational amplitudes are small. We do so because this kind of trajectories tends to be the most stable present in the system, a feature leading to conclude that the respective orbital de-stabilization may be connected with global spread of chaos throughout the phase space. The behavior of the fixed points as a function of the modulation amplitude ϵ may be accurately followed with help of a Newton-Raphson algorithm and the respective stability diagrams. In the stability diagrams one plots the so

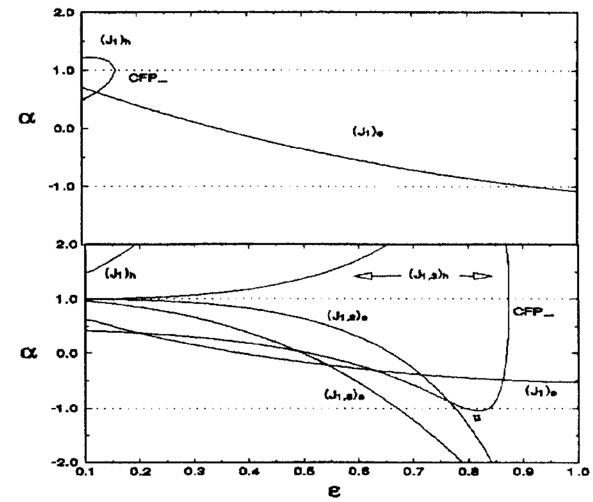

Figure 4: stability index vs. ϵ in the small (upper) and large Δ cases.

called stability index (α) of a particular periodic orbit as a function of the perturbing parameter. If $|\alpha| < 1$ the corresponding orbit is stable, if $|\alpha| > 1$ the orbit is unstable.

An important parameter that characterize the transition to chaos is the normalized detunning parameter defined as $\Delta_{\pm} \equiv (\omega_{\pm} - \Omega)/\omega_{\pm}$. Typical stability diagrams are show in fig. 4, where a comparision is made between the case of *small* and *large* Δ. One can see that when Δ is relatively small, only two stale fixed points of the mapping appear, one ceases to exists as it collapses with a neighboring unstable periodic orbit; the other undergoes an infinite cascade of period doubling bifurcations. When the frequency is large, the group contains more than two trajectories. The collapsing orbit behaves similarly as in the previous case. However, before it vanishes, it goes temporarily unstable within a band of the modulation amplitudes. Some of the other fail to undergo the period doubling sequence, a feature inhibiting global spread of chaos.

5 REFERENCES

[1] C. S. Roberts and S. J. Buchsbaum, Phys. Rev. **135**, 381 (1964).

[2] S. P. Kuo and G. Schimdt, J. Appl. Phys. **58**, 3646 (1985).

[3] C. Chen, Phys. Fluids **B3**, 2933 (1991) *and* Phys. Rev. A **46**, 6654 (1992).

[4] R. Pakter, R. S. Schneider and F. B. Rizzato, Phys. Rev. E **47**, 3787 (1993); Phys. Rev. E **49**, 1594 (1994)

[5] R. Shpitalnik, C. Cohen, F. Dothan, and L. Friedland, J. Appl. Phys. **70**, 1101 (1991).

[6] R. Pakter and F. B. Rizzato, Phys. Scripta, accepted (1993).

[7] A. C.-L. Chian and C. F. Kennel, Astrophys. Space Sci. **97**, 9 (1983).

[8] R. Pakter, G. Corso, T. S. Caetano, D. Dillenburg and F. B. Rizzato, Phys. Plasmas submitted (1994)